Key Engineering Materials
ISSN: 1662-9795, Vol. 988, pp 21-29
doi:10.4028/p-5c0LIi

Submitted: 2023-11-19
Revised: 2024-03-05
Accepted: 2024-03-08
Online: 2024-09-27

Hot Torsion Tests of AA6082 Alloy

Sara Di Donato[1,a*], Riccardo Pelaccia[2,b], Marco Negozio[1,c], Mohamad El Mehtedi[3,d], Barbara Reggiani[2,e], Lorenzo Donati[1,f]

[1]University of Bologna, DIN Department of Industrial Engineering, Viale Risorgimento 2, 40136 Bologna, Italy

[2]University of Modena and Reggio Emilia, Via Amendola 2, 42122 Reggio Emilia, Italy

[3]University of Cagliari, Via Marengo 2, 09123 Cagliari, Italy

[a]sara.didonato2@unibo.it, [b]riccardo.pelaccia@unimore.it, [c]marco.negozio2@unibo.it, [d]m.elmehtedi@unica.it, [e]barbara.reggiani@unimore.it, [f]l.donati@unibo.it

Keywords: Hot torsion test, Aluminum, Flow stress, Material characterization, AA6082.

Abstract. Materials characterization and the knowledge of their elastic-plastic behavior are of fundamental importance for the design of industrial manufacturing processes. Nowadays, FEM simulation is the main tool used to optimize product quality and minimize scraps, and the numerical codes have evolved over the years to obtain accurate solutions with reduced computational times. Nevertheless, in order to perform reliable simulations, it is necessary to include accurate modeling of the material flow stress.

Hot torsion is a powerful method for the characterization of the material flow stress because, tests can be carried out at constant speeds and temperatures, reaching large strain values, and thus getting over the limits of compression and tensile tests.

In this paper the hot torsion characterization applied to AA6082 alloy is presented: tests were performed with equivalent strain rates of 0.01, 0.1, 1, and 10 s^{-1}, in the temperature range from 440 to 550 °C (from 713.15 to 823.15 K). The results are presented in terms of equivalent stress vs equivalent strain.

Finally, the material flow stress curve was predicted by the Hyperbolic sine model and Hensel-Spittel law, and the material parameters A, $m_{1\text{-}9}$ are provided for the temperature expressed in °C and K.

Introduction

Finite Element Method is nowadays the most powerful tool for the design and optimization of the bulk-forming process. FEM codes have evolved over the years to gain accurate solving capabilities at reduced computational times, and this has led to a widespread diffusion of the numerical simulation tool in the manufacturing industry to improve product quality and reduce scraps. [1]

Especially in such sectors as aluminum extrusion, where on-plant experiments are complex and expensive for the complexity of the process, numerical simulation is of fundamental importance.

In the last few years, several research works have investigated different aspects of extrusion processes by means of FEM codes, from process and tool optimization to microstructure prediction, proposing different approaches and improving the accuracy of the simulation. [2, 3, 4, 5, 6, 7, 8]

In order to perform reliable and accurate simulations, it is necessary to provide the FEM code with accurate modeling of the material flow stress. In this sense, many equations over the years have been defined and included in the codes. Among these, in the past years, the Hyperbolic sine model proposed by Garafolo [9] was one of the most widespread and used. In fact, the Hyperbolic sine law, associated with the Zener-Hollomon parameter, allows the modelling of the material flow stress for a wide range of deformations conditions. [10, 11, 12, 13]

Nevertheless, the Hyperbolic sine law is a strain-independent model and could lead to large values of error in the simulation of plastic deformation processes where high strain values are reached.

A more accurate model for predicting the flow stress behavior of materials is the law proposed by Hensel-Spittel [14], which, including 9 material parameters, accounts for the dependence of flow stress on temperature, strain rate and strain. However, the limitation of the HS law is that the constitutive parameters are difficult to regress, and the related literature is lacking.

Furthermore, appropriate characterization tests of the material are necessary, which allow to reach large strain values, maintaining constant temperature and strain rate. In this context, the most effective test is the hot torsion test. A solid-bar or tubular specimen cylinder is twisted by a torque acting around its axis with constant speed and this allows it to reach extended strain values overcoming the limits of the tensile test, in which necking occurs characterizing the specimen up to strain about 0.5-0.8, and of the compression test, where the strain is limited to around 1 due to friction and barreling.

The aim of this work is to present the characterization of AA6082 aluminum alloy performed through hot torsion tests with the testing machine of the University of Bologna - Department of Industrial Engineering. Tests were carried out with equivalent strain rates of 0.01, 0.1, 1, and 10 s^{-1}, in the temperature range from 440 to 550 °C (from 713.15 to 823.15 K) and the results are presented in terms of equivalent stress vs equivalent strain.

Finally, the material flow stress curve was predicted by the Hyperbolic sine model and Hensel-Spittel law, and the material parameters A, $m_{1\text{-}9}$ are provided for the temperature expressed in °C and K.

Methodology and Experimental Procedures

Hot torsion test. The hot torsion tests were performed on AA6082 alloy homogenized solid-bar specimens. Although the torsion test has been used for many years, any standard doesn't exist for specimen design, and researchers all over the years tried to use different geometries for the specimens with a gauge-length-to-radius ratio approximately from 0.63:1 to 17:1. [11, 12, 13, 15, 16]

In general, the design of the sample, including the shoulder and grip ends, is determined largely by the method of heating and the type of torsion machine to be used. In this work, a specimen with a gauge length and a diameter of 10 mm was used, as shown in Fig. 1 a.

During the test, the temperature, measured by a thermocouple inserted inside the specimen, is kept constant by a PID controller. The samples were heated at approximately 1.5 °C/s by means of a copper induction coil (Fig. 1 b) and maintained for 5 minutes at the testing temperature before torsion, in order to allow a homogeneous temperature distribution from the external diameter to the center.

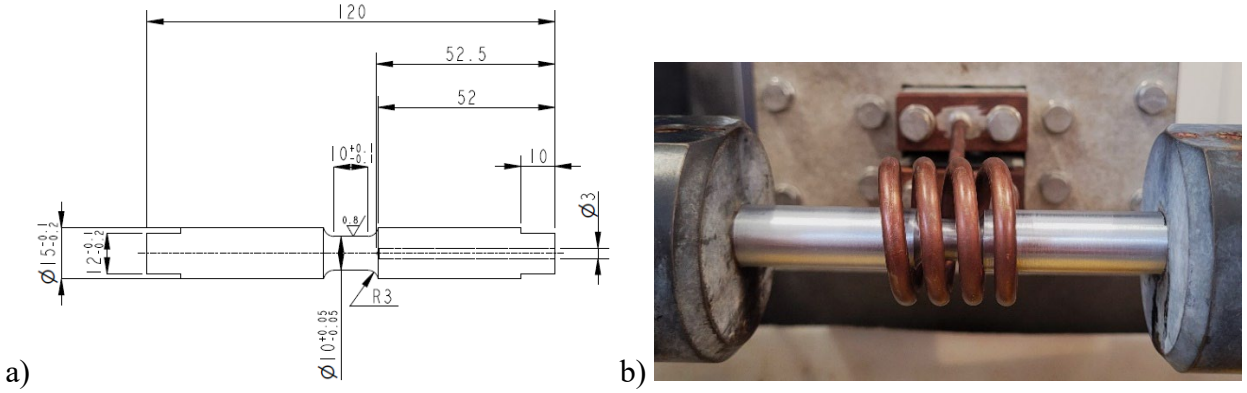

a) b)

Fig. 1. a) Geometry of the AA6082 alloy solid bar specimen with dimensions in mm; b) Picture of the sample during the test performed with the Torsion testing machine of the University of Bologna - Department of Industrial Engineering.

The torsion test provides the relationship between the angular deformation applied to the sample and the torque required to obtain it. The outputs of the test machine are the torque M [N·m] and the angle of twist θ [rad]. The Fields-Backofen solution was applied to calculate the shear strain and the corresponding shear stress [17]. Applying this method, the shear strain in the relation τ-γ and the shear strain rate are considered to be those corresponding to the outside diameter of the solid bar sample (Eq. 1, Eq. 2).

$$\gamma = \frac{R\,\theta}{L}\ , \tag{1}$$

$$\dot{\gamma} = \frac{R\,\dot{\theta}}{L}\ , \tag{2}$$

where L is the gauge length of the specimen (10 mm) and R is the radius (5 mm). Fig. 2
The shear stress is calculated from Eq. 3:

$$\tau = \frac{M}{2\,\pi\,R^3}(3 + n + m)\ , \tag{3}$$

where the strain hardening coefficient *n* is the instantaneous slope of logM versus logθ and the strain rate sensitivity coefficient *m* is the slope of logM versus log$\dot{\theta}$ at fixed values of θ. Several studies demonstrated that the effects of m and n coefficients can be neglected for aluminum alloys to simplify the stress calculation, as they don't significantly affect the material behavior. [11, 12, 13, 18, 19]

In the present work, the equivalent Von Mises stress and strain were calculated neglecting the effects of m and n coefficients according to Eq. 4 and Eq. 5.

$$\bar{\sigma} = \frac{M\,3\sqrt{3}}{2\,\pi\,R^3}\ , \tag{4}$$

$$\bar{\varepsilon} = \frac{\gamma}{\sqrt{3}}\ . \tag{5}$$

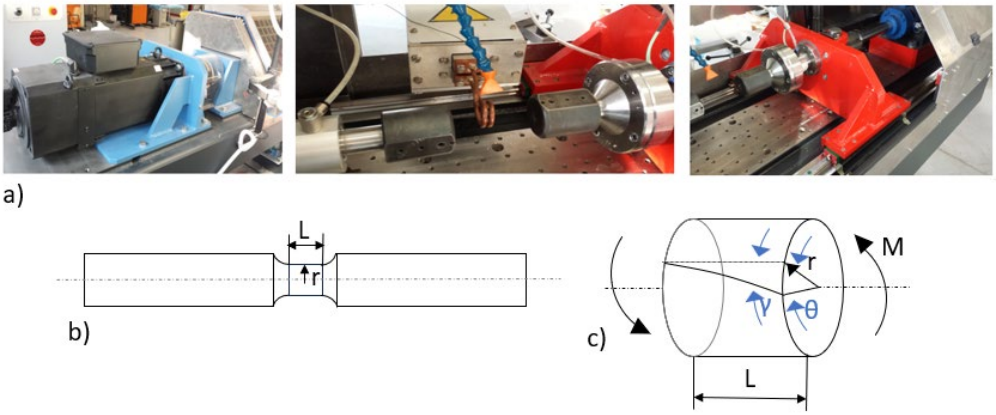

Fig. 2. a) Picture of the Torsion testing machine of the University of Bologna - Department of Industrial Engineering; b) Scheme of the specimen; c) Scheme of the shear strain on the gauge length.

Results and Discussion

Experimental results. Fig. 3 shows the experimental results in the form of equivalent stress vs equivalent strain calculated by Eq 4 and Eq. 5. The tests were carried out with equivalent strain rates of 0.01, 0.1, 1, and 10 s^{-1}, maintaining four temperature values, 440, 480, 520, and 550 °C; for each condition, at least two trials were performed to verify the repeatability of the test.

The curves have the typical shape of many aluminum alloys behavior, with a peak at low strains followed by a softening steady state. The tests were stopped after the specimens fractured which occurred over an equivalent strain equal to 5 for most conditions.

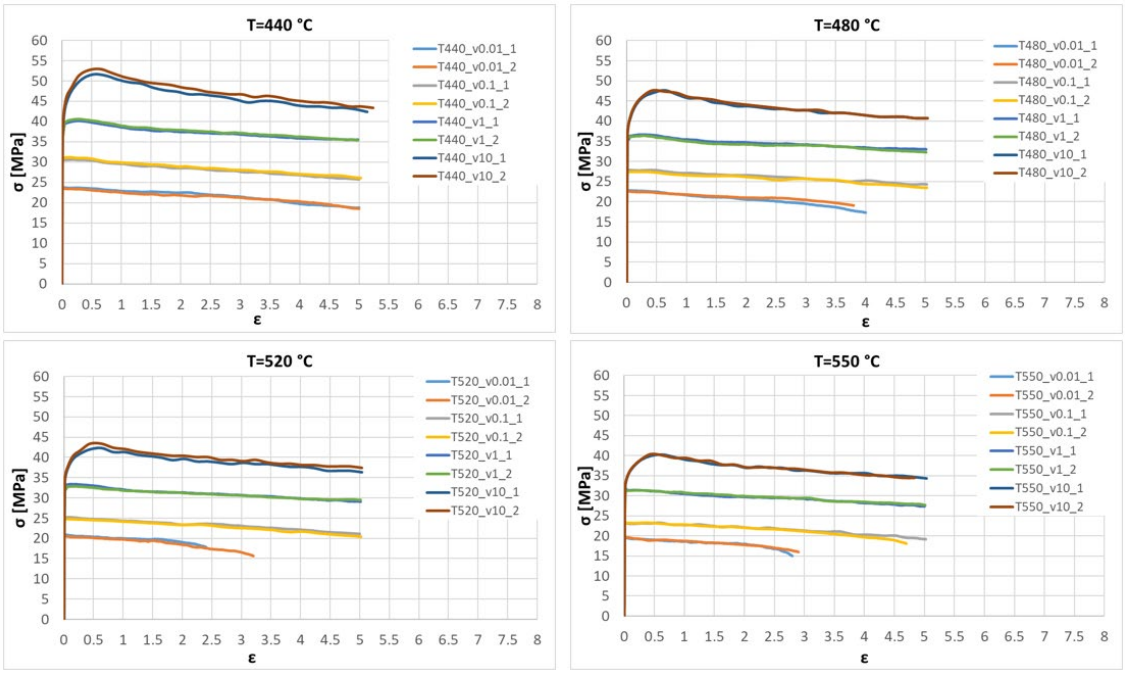

Fig. 3. Experimental σ-ε curves. The tests were performed with four values of temperature: 440, 480, 520 and 550 °C, and four values of strain rates: 0.01, 0.1, 1, and 10 s^{-1}. For each condition two trials were carried out.

Hyperbolic sine law. The hyperbolic sine law is a model proposed by Garofalo [9] which, associated with the Zener-Hollomon parameter, allows the modelling of the material flow stress for a wide range of deformations conditions [10, 11, 12, 13]. The expression describes the flow stress dependence on temperature and strain rate, without considering the strain, and assumes the following form: Eq. 6

$$\bar{\sigma} = \frac{1}{a}\sinh^{-1}\left[\left[\frac{1}{A}\dot{\varepsilon}\exp\left(\frac{Q}{RT}\right)\right]^{\frac{1}{n}}\right] = \frac{1}{a}\sinh^{-1}\left[\left(\frac{Z}{A}\right)^{\frac{1}{n}}\right], \quad (6)$$

with stress $\bar{\sigma}$ expressed in MPa and temperature T expressed in K. R is the universal gas constant (8.314 J/mol·K), Q is the apparent activation energy for plastic flow, A, α, and n are material constants.

The values of the material parameters were found from the hot torsion tests' experimental results, considering the peak stress value for each condition and they are reported in Table 1.

Table 1. Sin-hyperbolic model parameters.

Q [J/mol]	A [s^{-1}]	α [MPa^{-1}]	n
103639.3118	7.95 E+04	0.045	5.49933

Fig. 4 shows the comparison between the experimental flow stress curves plotted with dashed lines and the predicted stress values, calculated by Eq. 6, drawn with solid lines. It's clear that the curves calculated with the Hyperbolic sine law appear constant as the strain varies and the correlation is good only for the peak stress values as shown in Fig. 5, except for the test conditions with the strain rate of 0.01 s^{-1} and temperature of 793 and 823 K, where the predicted peak stress is lower than the experimental peak.

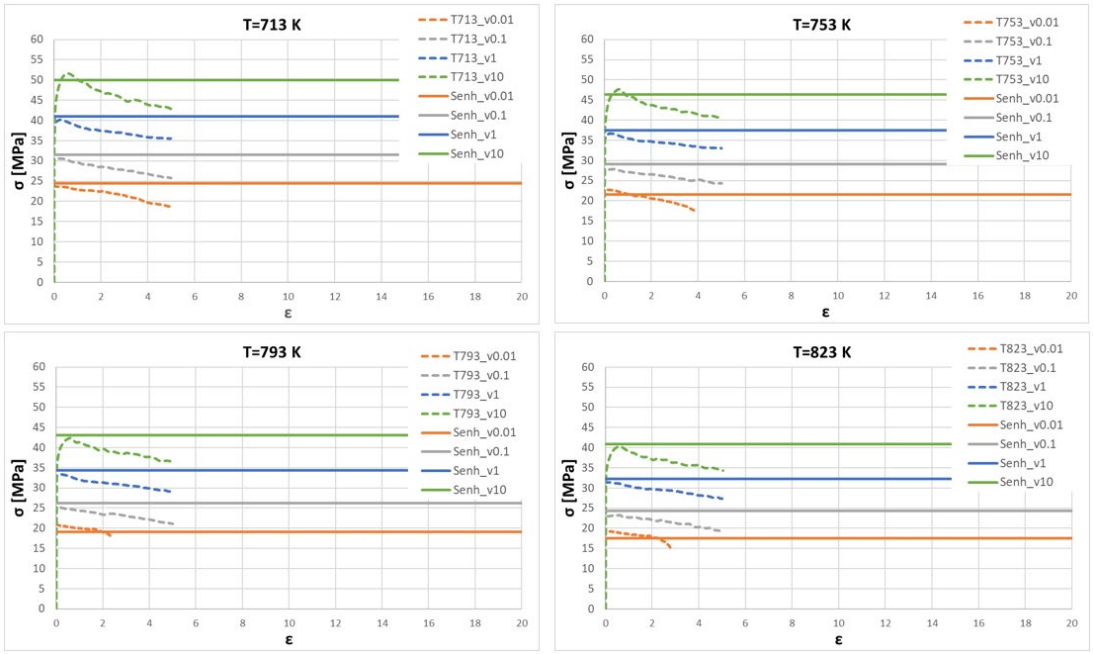

Fig. 4. Comparison between the experimental σ-ε curves (dashed lines) and the stress values predicted by Sinh law (solid lines).

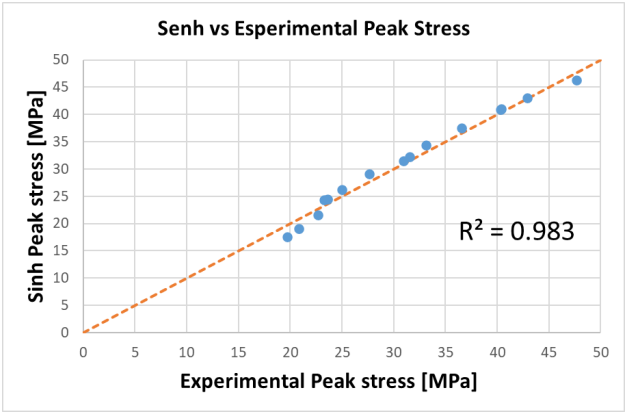

Fig. 5. Comparison between peak stress values predicted by Sinh law on the y-axis and the experimental peak stress values on the x-axis. The orange dashed line represents the alignment between the predicted and experimental data and indicates a theoretically perfect level of agreement between the values.

Hensel and Spittel law. The Hensel and Spittel law [14] is a model for predicting material flow stress behavior involving temperature, strain rate and strain dependence. The equation, described in Eq. 7, contains 9 material parameters: A, m_1, m_2, m_3, m_4, m_5, m_7, m_8, m_9,

$$\bar{\sigma} = A\, e^{m_1 T} \bar{\varepsilon}^{m_2} \dot{\bar{\varepsilon}}^{m_3} e^{\frac{m_4}{\bar{\varepsilon}}} (1+\bar{\varepsilon})^{m_5 T} e^{m_7 \bar{\varepsilon}} \dot{\bar{\varepsilon}}^{m_8 T} T^{m_9}. \quad (7)$$

Where $\bar{\sigma}$ is expressed in MPa and the coefficients assume different values depending on whether the temperature is expressed in °C or K. The coefficients m_1 and m_9 define the material's sensitivity to temperature, m_5 defines the coupling temperature and strain, the term m_8 couple temperature and strain rate, m_2, m_4, and m_7 coefficients define the material's sensitivity to strain and m_3 depends on the material's sensitivity to strain rate. [20, 21]

The values of the coefficients were found from the hot torsion tests' experimental results and are listed in Table 2 for the temperature expressed in K and in Table 3 for the temperature expressed in °C.

Table 2. Hensel-Spittel coefficients with temperature expressed in K (Temperature range validity 713-823 K).

Parameters	5 parameters	6 parameters	7 parameters	8 parameters	9 parameters
A [MPa]	182.562	176.285	178.685	182.161	87.963
m1	-0.0022426	-0.0023064	-0.0023004	-0.00215	-0.0035864
m2	-0.0405691	-0.0610555	-0.0542036	0.008047	0.0081011
m3	0.105639	0.1052751	0.1062478	-0.02175	-0.0225208
m4	-0.0012775	-0.0012881	-0.00121413	-0.00029	-0.00029223
m5	0	7.54071E-05	5.60459E-05	-7.2E-05	-7.215E-05
m7	0	0	-0.0003077	0.000282	0.0002987
m8	0	0	0	0.000142	0.0001588
m9	0	0	0	0	0.2766873
R^2	0.972	0.960	0.965	0.969	0.939

Table 3. Hensel-Spittel coefficients with temperature expressed in °C (Temperature range validity 440-550 °C).

Parameters	5 parameters	6 parameters	7 parameters	8 parameters	9 parameters
A [MPa]	98.851	96.259	107.028	99.774	99.722
m1	-0.0022408	-0.0023101	-0.0022578	-0.00212	-0.00212
m2	-0.0405691	-0.0550745	0.0074409	0.007399	0.007401
m3	0.105639	0.105639	0.0880616	0.017222	0.017216
m4	-0.0012775	-0.00128502	-0.0002925	-0.00029	-0.00029
m5	0	0.00009201	-0.00010522	-0.0001	-0.0001
m7	0	0	6.43551E-05	2.35E-05	2.37E-05
m8	0	0	0	0.000142	0.000142
m9	0	0	0	0	9.33E-05
R^2	0.972	0.965	0.970	0.968	0.968

The H-S law can be used in a simplified form, using only 5 material coefficients, or getting all 9 of them. For the AA6082 alloy tested in the present work, it was found that the stresses predicted by using the Hensel-Spittel law with 5 coefficients present an excellent agreement with the experimental stresses, as shown in Fig. 6, where the comparison between the experimental flow stress curves plotted with dashed lines and the predicted stress values, expressed in K, drawn with solid lines, is shown. By increasing the number of coefficients, the agreement between the predicted flow stress and the experimental one gets worse, causing a decrease in the R^2 from a value of 0.972 for the H-S law with 5 coefficients to a value of 0.939 for the H-S law with 9 coefficients, as shown in Fig. 7 and Fig. 8. The same considerations can be made for the values of the Hensel-Spittel coefficients expressed in °C.

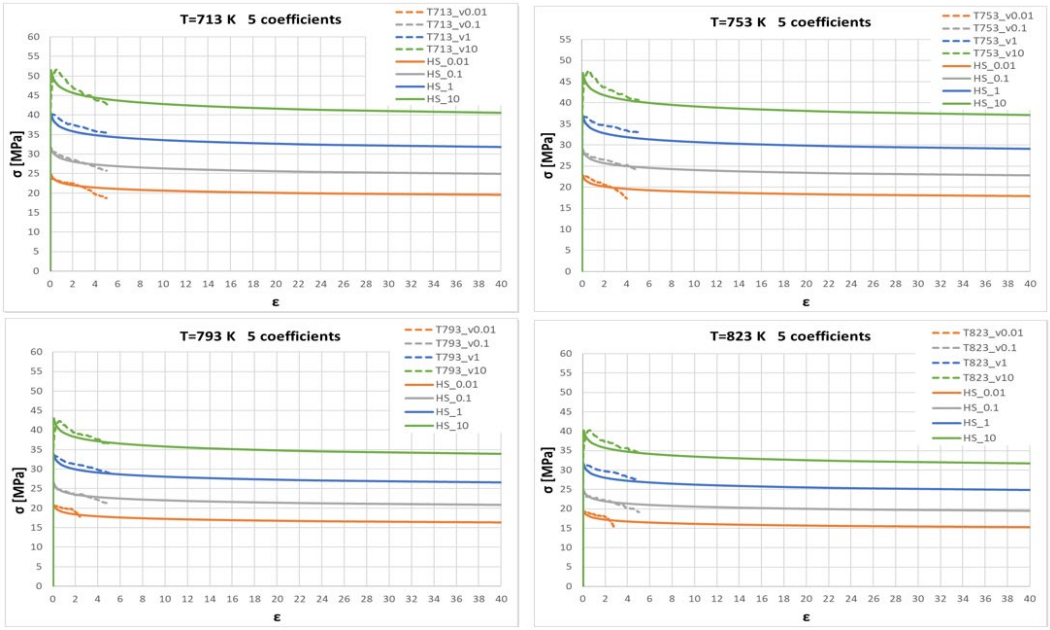

Fig. 6. Comparison between the experimental σ-ε curves (dashed lines) and the stress values predicted by Hensel-Spittel law with 5 coefficients: A, m_1, m_2, m_3, m_4 (solid lines).

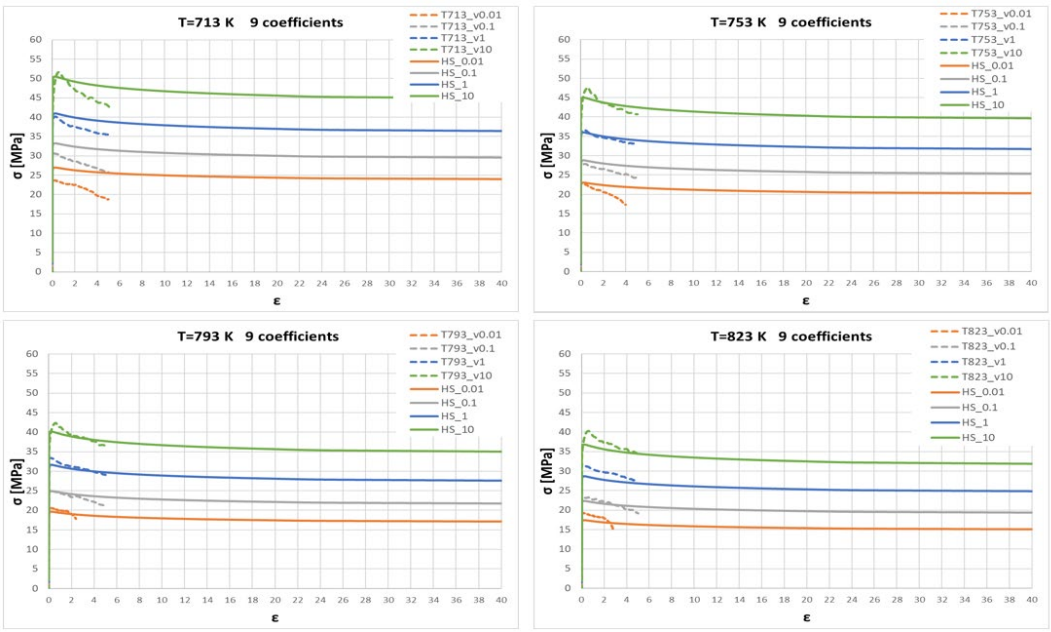

Fig. 7. Comparison between the experimental σ-ε curves (dashed lines) and the stress values predicted by Hensel-Spittel law with 5 coefficients: A, m_1, m_2, m_3, m_4, m_5, m_7, m_8, m_9 (solid lines).

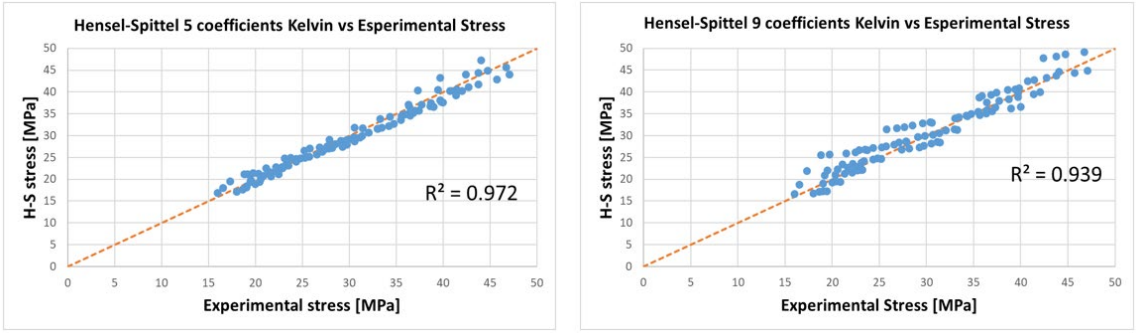

Fig. 8 Comparison between stress values predicted by Hensel-Spittel law on the y-axis and the experimental stress values on the x-axis (with 5 coefficients on the left and 9 coefficients on the right). The orange dashed line represents the alignment between the predicted and experimental data and indicates a theoretically perfect level of agreement between the values.

Conclusions

In this paper, the AA6082 alloy's plastic behaviour was characterised and analysed by means of the hot torsion test performed with the testing machine of the University of Bologna - Department of Industrial Engineering. The trials were carried out applying four strain rate values 0.01, 0.1, 1, and 10 s^{-1}, and four temperatures 440, 480, 520, and 550 °C (713, 753, 793 and 823 K). At least two tests were performed for each condition showing good repeatability of the results.

Two constitutive flow stress models for the tested alloy were investigated: the Hyperbolic sine law and the Hensel-Spittel law. The models were regressed from the hot torsion tests' experimental results and the material coefficients were provided. The Hyperbolic sine law is a strain-independent model and it exhibited good accuracy in predicting peak stress values. The Hansel-Spittel law includes 9 parameters that account for the dependence of material flow stress on temperature, strain rate, and strain. In the present work, the Hansel-Spittel parameters were provided both for the temperatures expressed in K and in °C. It was found that the stresses predicted by using the H-S model with 5 coefficients showed better agreement with the experimental data than the stresses calculated by H-S model with 6, 7,8, and 9 parameters respectively.

Acknowledgments

The authors would like to strongly acknowledge all the Companies and persons that made possible to carry out the experiment. In particular, the authors acknowledge the operators and the plant director Eng. Luca Gorlani from Metra plant in Rodengo Saiano (BS, Italy) for the supply of material and the press usage, and Almax Mori Group (TN, Italy), in particular Eng. Tommaso Pinter, for the die design and manufacturing. All these companies and involved persons are strongly acknowledged for their kind support, activity and problem-solving approach.

Funding

National Recovery and Resilience Plan (NRRP), Mission 04 Component 2 Investment 1.5-NextGenerationEU, Call for tender n.3277 dated 30/12/2021 (Award Number: 0001052 dated 23/06/2022).

References

[1] L. Donati, B. Reggiani, R. Pelaccia, M. Negozio, S. Di Donato, Advancements in extrusion and drawing: a review of the contributes by the ESAFORM community, International Journal of Material 15 41 (2022).

[2] L. Donati, A. Segatori, M. El Mehtedi, L. Tomesani, Grain evolution analysis and experimental validation in the extrusion of 6XXX alloys by use of a lagrangian FE code, International Journal of Plasticity 46 (2013) 70-81.

[3] R. Pelaccia, B. Reggiani, M. Negozio, L. Donati, Liquid nitrogen in the industrial practice of hot aluminium extrusion: experimental and numerical investigation, Int J Adv Manuf Technol 119 (2022) 3141-3155.

[4] M. Negozio, R. Pelaccia, L. Donati, B. Reggiani, FEM Analysis of the Skin Contamination Behavior in the Extrusion of a AA6082 Profile, Key Engineering Materials Trans Tech Publications Ltd. (July 22, 2022).

[5] R. Pelaccia, B. Reggiani, M. Negozio, S. Di Donato, L. Donati, Investigation on the topological optimization of cooling channels for extrusion dies, Materials Research Proceedings 28 (2023) 533-542.

[6] I. Kniazkin, R. Pelaccia, M. Negozio, S. Di Donato, L. Donati, B. Reggiani, N. Biba, R. Rezvykh, I. Kulakov, Investigation of the skin contamination predictability by means of QForm UK extrusion code, Materials Research Proceedings 28 (2023) 543-552.

[7] M. Negozio, L. Donati, R. Pelaccia, B. Reggiani, S. Di Donato, Experimental analysis and modeling of the recrystallization behaviour of a AA6060 extruded profile, Materials Research Proceedings 28 (2023) 477-486.

[8] M. Negozio, R. Pelaccia, L. Donati, B. Reggiani, Simulation of the microstructure evolution during the extrusion of two industrial-scale AA6063 profiles, Journal of Manufacturing Processes 99 (2023) 501-512.

[9] F. Garofalo, An empirical relation defining the stress dependence of minimum creep rate in metals, Transactions of the Metallurgical Society of Aime 227 (April 1963) 351-356.

[10] C.M. Sellars, WJ McG Tegart, Memoires Scientifique Rev. Metallurg. 58 9 (1966) 731.

[11] G.E. Dieter, S.L. Semiatin, H.A. Kuhn, Handbook of Workability and Process Design, ASM International publications United States of America (2003) 86-127.

[12] L. Donati, M. El Mehtedi, Characterization of Flow Stress of Different AA6082 Alloys By Means Of Hot Torsion Test, AIPConf Proc 1353 (2011) 455-460.

[13] M. El Mehtedi, S. Spigarelli, F. Gabrielli, L. Donati, Comparison Study of Constitutive Models in Predicting the Hot Deformation Behavior of AA6060 and AA6063 Aluminium Alloys, Materials Today: Proceedings 2 10 Part A (2015) 4732-4739.

[14] A. Hensel, T. Spittel, Kraft- und Arbeitsbedarf bildsamer Formgebungsverfahren, Deutscher Verlag für Grundstoffindustrie: Leipzig, Germany (1978) 336-360.

[15] G.R. Canova, U.F. Kocks, J.J. Jonas, Theory of torsion texture development, Acta metall. 32 2 (1984) 211-226.

[16] A. Gräber, K. Pöhlandt, State of the art of the torsion test for determining flow curves, Steel Res. 61 (1990) 212-218.

[17] D.S. Fields, W.A. Backofen, Determination of strain-hardening characteristics by torsion testing, 57 (1957) 1259-1272.

[18] B. Verlinden, A. Suhadi, L. Delaey, A generalized constitutive equation for an AA6060 Aluminium alloy, Scripta Metallurgica et Materialia 28 11 (1993) 1441-1446.

[19] S. Spigarelli, E. Evangelista, H.J. McQueen, Study of hot workability of a heat treated AA6082 aluminum alloy, Scripta Materialia 49 (2003) 179-183.

[20] X. Chen,Y. Du, K. Du, T. Lian, B. Liu, Z. Li, X. Zhou, Identification of the Constitutive Model Parameters by Inverse Optimization Method and Characterization of Hot Deformation Behavior for Ultra-Supercritical Rotor Steel, Materials 14 8 (2021) 1958.

[21] H. Wang, W. Wang, R. Zhai, R. Ma, J. Zhao, Z. Mu, Constitutive Equations for Describing the Warm and Hot Deformation Behavior of 20Cr2Ni4A Alloy Steel, Metals. 10 9 (2020) 1169.